 doi:10.20944/preprints201708.0101.v1

The significance of infiltration and spatial variability of rainfall on the numerical reproduction of urban floods

Laurent G. Courty[1,*], Miguel A. Rico-Ramirez[2] and Adrián Pedrozo-Acuña[1]

[1] *Instituto de Ingeniería, Universidad Nacional Autónoma de México, Mexico city*
[2] *Department of Civil Engineering, University of Bristol, UK*
[*] *Correspondence to: lcourty@ii.unam.mx*

Keywords: floods, radar rainfall, kriging, computer modelling

August 28, 2017

The growth of urban population, combined with an increase of extreme events due to climate changes call for a better understanding and representation of urban floods. Rainfall and infiltration are two important factors that affect the watershed response to a given precipitation event. In this paper, we evaluate the influence of the representation of infiltration and spatially variable rainfall on the computer simulation of the floods that affected the city of Hull, UK in June 2007. This work compares a uniform rainfall with one generated using Kriging with External Drift and a constant infiltration equal to the soil hydraulic conductivity with a neglected infiltration. The results of the four simulations are then compared with the flood extents observed by public authorities. It results that the computer model is able the reproduce the general dynamic of the flood and identify the main inundated areas. We found that neglecting the infiltration induce a better representation of this flood event. Furthermore, the use of radar rainfall results in an accuracy similar to the one obtained with a constant rainfall. This study indicates that when the spatial resolution of the rainfall data is low compared to the catchment size and the precipitation distribution is uniform, the spatial variability of the rainfall might not add significant information.

1 Introduction

With the advent of computational methods and computer processing power, the ability to tackle urban floods at a catchment level is clearly emerging, making it possible to apply an integrated approach to

 doi:10.20944/preprints201708.0101.v1

modelling rainfall-runoff processes along with surface flows (Yu and T. J. Coulthard, 2015; Courty et al., 2017). Moreover, the availability of new data sources with higher quality and resolution (e.g. radar derived precipitation data and lidar derived terrain data) enable the utilisation of a modelling approach which is closer to what happens in the real world.

On the other hand, the documented growth in the number of floods and urban population due to climate change (Hirabayashi et al., 2013), clearly indicate the importance of an improved understanding on how the flood waters interact with urban environment both in space and time. The development of a reliable approach to adequately describe urban flood processes has been recognised as a challenging task (Vojinović and Abbott, 2012).

Recent advances in urban flood modelling recognise the importance of 2D modelling algorithms to adequately reproduce urban floods (Hunter et al., 2008). However, it should be borne in mind that model performance also depends on the quality of data utilised to define the topography and forcing conditions that give birth to an urban flood. Therefore, hydrological processes should be considered to an adequate level of complexity related to the urban catchment where they occur.

Among the main factors identified to adequately reproduce floods are the terrain model, the amount of precipitation, the infiltration and the friction. Both rainfall and infiltration influence the amount of effective rainfall that produce surface flows. Indeed, the spatial variability of rainfall has been recognised as an essential property to model floods in urbanised watersheds (Segond et al., 2007; Bruni et al., 2015; M. Rico-Ramirez et al., 2015; Cristiano et al., 2017). In contrast, with regards to the infiltration, Leandro et al. (2016) noted that this process is usually neglected or considered by means of a constant rate in the best case. This simplification is mainly ascribed to the low importance of infiltration in impervious urban areas and to an interest focused in extreme scenarios when soil is saturated. However, if a whole catchment approach is considered to model urban flows, it may be necessary to define infiltration rates at the relevant spatial scale (e.g. rural land within the catchment). Therefore, a more realistic representation of urban floods should include not only the definition of flows within the city, but also those coming from the rest of the contributing catchment, which require a spatially variable infiltration rate defined in relation to the soil type found in rural areas.

A good and documented example of an urban flood in the real world was registered in the United Kingdom on June 25th 2007, when the city of Kingston upon Hull (herein later referred to as Hull), East Yorkshire, suffered heavy flooding that affected 8600 homes and 1300 businesses (T. Coulthard and Frostick, 2010). Although the numerical reproduction of this event has been reported in Yu and T. J. Coulthard (2015) or Courty et al. (2017), a realistic definition of the model setup has not been discussed or attempted. For instance, with regards to the infiltration process, Yu and T. J. Coulthard (2015) presented a sensitivity analysis of various drainage capacities and hydraulic conductivity values with their effects on model skill when compared to reference numerical derived flood maps. Moreover, the spatial resolution at which the model was implemented (10m and 20m) may be considered coarse for an urban flood modelling exercise. Courty et al. (2017) used a similar numerical approach to Yu and T. J. Coulthard (2015), but neglected the infiltration and used a spatial resolution of 5m given by the LiDAR derived Digital Elevation Model (DEM). Both numerical approaches resolve the inertial equation proposed by Bates et al. (2010), incorporating the Green–Ampt formula to simulate the infiltration process, differing only in the way the adaptive time-step is implemented. Notably, in both studies, rainfall was considered using hourly measurements of only one rain-gauge located at Hull University. Therefore, the precipitation was assumed to be spatially uniform within the catchment. This constraint may cast some doubt on the adequacy of the numerical representation of rainfall, which lacks a realistic representation of its spatial distribution during the event.

It is well known that a good knowledge of precipitation at appropriate spatial and temporal scales enhances modelling of rainfall-runoff processes in urban catchments (Segond et al., 2007; Bruni et al., 2015; M. Rico-Ramirez et al., 2015; Cristiano et al., 2017). Accurate estimations of precipitation in urban areas require a dense rain gauge network combined with an effective analysis method. However, rain gauge networks are generally too sparse spatially to provide such detailed information (Seo, 1998). On the other hand, information acquired with weather radars enable a better spatial description of rainfall fields, but also lack a proper spatial resolution for urban applications with grids of 2 km or coarser

Preprints (www.preprints.org) | NOT PEER-REVIEWED | Posted: 29 August 2017 doi:10.20944/preprints201708.0101.v1

(Nesbitt and Anders, 2009; Smith, Baeck, et al., 2007). Furthermore, weather radar measurements are inherently uncertain to some degree, as the relationship between reflectivity and actual rainfall on the ground requires the derivation of empirical coefficients (Smith and Krajewski, 1993). An alternative way of making use of this data is to blend rain gauge and weather radar data (Ercan and Goodall, 2013; Goudenhoofdt and Delobbe, 2009; Velasco-Forero et al., 2009).

Although it is known that spatially detailed and accurate rainfall data remain a limiting factor in urban flood studies (Hill et al., 2014), it is necessary to further advance our knowledge on how these different approaches to the definition of a rainfall field improve or not results of urban flood modelling studies, comparing for instance the affected areas determined during a severe flood.

The purpose of this study is to investigate how a better definition of the spatial variability of rainfall and hydraulic conductivity improve the results of a urban flood modelling exercise. For this, we utilise the case study from the severe floods registered in Hull, UK in 2007. Flood maps derived from the use of a uniform rainfall field against those resulting from a merged product from weather radar and rain gauge data will be compared and discussed. Focus will be given to the west part of the city of Hull, which was the most affected according to T. Coulthard and Frostick (2010).

This paper is organised as follows, Section 2 introduces the flood inundation model use to replicate this event as well as the forcing data required to run the model; Section 3 presents the results from a qualitatively and quantitative perspective; Section 4 discusses the outcomes in light of similar studies and summarises the main conclusions derived from this investigation.

2 Materials and methods

2.1 Computer model

We use Itzï, an open-source fully distributed dynamic hydrologic and hydraulic model based on Geographical Information System (GIS). We will here present briefly the model. A more complete description can be found in Courty et al. (2017). Itzï solve the partial inertia approximation of the Barré de Saint-Venant Equations (SVE) by applying an explicit finite-difference scheme to a regular raster grid (Almeida, Bates, et al., 2012; Almeida and Bates, 2013).

The time-step duration Δt is calculated at each time-step using Eq. 1, where h_{max} is the maximum water depth within the domain, g the acceleration due to the gravity, Δx and Δy the cell dimensions in m and α an adjustment factor.

$$\Delta t = \alpha \frac{\min\{\Delta x, \Delta y\}}{\sqrt{g \times h_{max}}} \tag{1}$$

The specific flow between cells q in $\mathrm{m^2\,s^{-1}}$ is calculated using Eq. 2.

$$q_{i+1/2}^{t+\Delta t} = \frac{\left(\theta q_{i+1/2}^{t} + (1-\theta)\frac{q_{i-1/2}^{t} + q_{i+3/2}^{t}}{2}\right) + g h_f \Delta t S}{1 + g \Delta t n^2 ||q_{i+1/2}^{t}|| / {h_f}^{7/3}} \tag{2}$$

where subscripts i and t denotes space and time indices, S the hydraulic slope, n the Manning's number in $\mathrm{s\,m^{-1/3}}$ and θ an inertia weighting factor. The flow depth h_f is the difference between the highest water surface elevation y and the highest terrain elevation z. It is used as an approximation of the hydraulic radius.

The new water depth at each cell is calculated using Eq. 3. It is the sum of the current depth h^t, the external factors h_{ext}^t (rainfall, infiltration, drainage etc.) and the flows passing through the four faces of each cell $Q_{i,j}^t$.

$$h^{t+\Delta t} = h^t + h_{ext}^t + \frac{\sum^4 Q_{i,j}^t}{\Delta x \Delta y} \times \Delta t \tag{3}$$

Preprints (www.preprints.org) | NOT PEER-REVIEWED | Posted: 29 August 2017 doi:10.20944/preprints201708.0101.v1

Table 1: *Features comparison between LISFLOOD-FP, FloodMap and Itzï*

Feature	LISFLOOD-FP	FloodMap	Itzï
Flow equation	Damped partial inertia[1]	Partial inertia[2]	Damped partial inertia[1]
Adaptive time-step	Global	Local	Global
1D River model	Yes	Yes	No
Infiltration model	No	Green–Ampt	Green–Ampt
GIS integration	Loose	Loose	Tight
Spatio-temporal variability of input	No	No	Yes
Free Software	No[3]	No	Yes (GNU GPL)
Parallel processing	OpenMP	MPI	OpenMP

[1] Almeida, Bates, et al. (2012), Almeida and Bates (2013)
[2] Bates et al. (2010)
[3] Although Glofrim (`https://github.com/openearth/glofrim`) contains LISFLOOD-FP and is released under the GNU GPL, its README says "Please note that the downloadable LISFLOOD-FP version is not meant for further unauthorized distribution", which places LISFLOOD-FP outside the scope of the license.

The infiltration could be represented either by a time-series of maps of user-defined value, or by using the Green–Ampt formula, shown in Equation (4). Where f is the infiltration rate ($\mathrm{m\,s^{-1}}$), K the hydraulic conductivity ($\mathrm{m\,s^{-1}}$), θ_e the effective porosity in ($\mathrm{m\,m^{-1}}$), θ the initial water soil content ($\mathrm{m\,m^{-1}}$), ψ_f the wetting front capillary pressure head (m) and F the infiltration amount (m).

$$f = K\left(1 + \frac{(\theta_e - \theta)\psi_f}{F}\right) \tag{4}$$

Itzï can model the capacity of the sewer system by accounting for losses in $\mathrm{mm\,h^{-1}}$. Those losses are accounted for in the same way as the infiltration, during the calculation of the new water depth in each cell (See Eq. 3).

The numerical scheme used by Itzï is similar to the one used by FloodMap-HydroInundation2D (Yu and T. J. Coulthard, 2015) and the inertial solver of LISFLOOD-FP (Almeida, Bates, et al., 2012; Almeida and Bates, 2013). For instance Itzï uses the same numerical scheme than the inertial solver of LISFLOOD-FP, and produces virtually identical results (Courty et al., 2017). However, those three models present significant differences recapitulated in Table 1. Notably, the tight integration of Itzï with Geographic Resources Analysis Support System (GRASS)—an open source GIS software (Neteler et al., 2012)—allows the use of raster time-series for any entry data. In the present case, this capacity is used for the representation of the radar rainfall.

2.2 Entry data

For this study we use a Digital Elevation Model (DEM) obtained from aerial Light Detection And Ranging (LiDAR). Its spatial resolution is 5 m. It can be see in Fig. 1 that the study area could be divided in two zones. The western part is a hillside while the eastern part is mostly flat with some areas below the mean sea level. The constructed area is concentrated in the flat eastern part.

After the event, the Hull City Council (HCC) and the Environment Agency of the United Kingdom (EA) evaluated the extension of the affected areas. While the EA used aerial photography to map the flooded areas, the HCC carried out a poll among the residents (T. Coulthard and Frostick, 2010). The areas identified by each administration are represented in Fig. 2. It could be noted that the two zones classified by the two administrations shows significant differences highlighted in Table 2. Notably, less than half of the individual observations could be validated by the other. Furthermore, due to the limitations of the collection methods, it is possible that the identification of the flooded areas is partial and that some actually affected areas might not be represented (T. Coulthard and Frostick, 2010).

The Manning's n friction map is created using the Global Land Cover (GLC30) map from the National Geomatics Center of China (Chen et al., 2014). Figure 3 shows the map of the repartition of the land

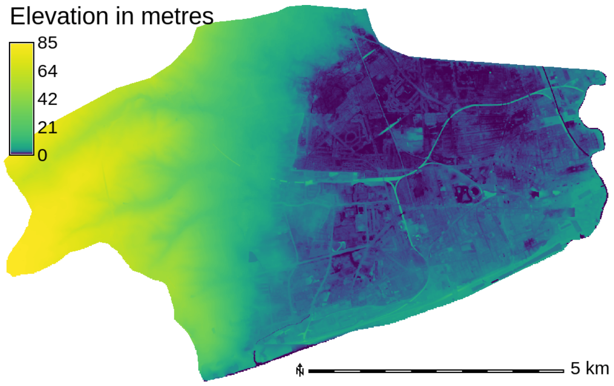

Figure 1: *Digital Elevation Model of the study area*

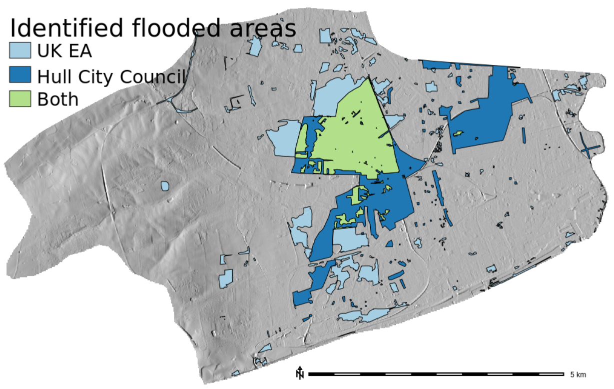

Figure 2: *Identified flooded areas. Light blue: EA only. Dark blue: HCC only. Green: Intersection of both administrations.*

Table 2: *Comparison of identified flood extents*

Collecting entity	Area (km^2)
Environment Agency	5.16
Hull City Council	6.18
Intersection of both	2.33

Preprints (www.preprints.org) | NOT PEER-REVIEWED | Posted: 29 August 2017 doi:10.20944/preprints201708.0101.v1

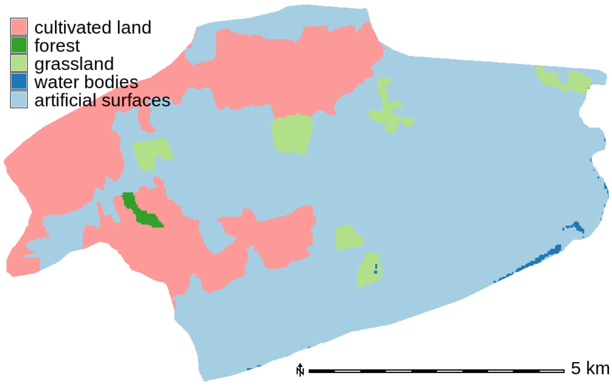

Figure 3: *Land cover classes from Global Land Cover in the study area*

Table 3: *Relation between land cover classes and Manning's n values.*

GLC30 class	Category from Chow (1959)	Manning's n ($\mathrm{s\,m^{-1/3}}$)
Cultivated land	Mature field crops	0.040
Forest	Cleared land with tree stumps, heavy growth of sprouts	0.060
Grassland	Pasture with short grass	0.030
Water bodies	Natural stream: clean, straight, full stage, no rifts or deep pool	0.030
Artificial surfaces	Gunite, good section	0.019

cover classes over the study area. Typical values of n from the literature are assigned for each cell according to its class (Chow, 1959). Table 3 shows the relation between the land cover classes and the Manning's n values proposed by Chow (1959).

The drainage of the city of Hull is entirely pumped because of the topographic situation of the urban area (T. Coulthard and Frostick, 2010). The drainage of the study area was carried out by the combined action of the following pumping stations that worked continuously during the event (T. Coulthard and Frostick, 2010):

- West Hull pumping station (capacity $32\,\mathrm{m^3\,s^{-1}}$), draining the whole study area plus a smaller part of the city north of it.
- Saltend Waste Water Treatment Work (outflow $22\,\mathrm{m^3\,s^{-1}}$), treating most of Hull, including the study area.

Yu and T. J. Coulthard (2015) mention drainage capacity values for Hull of $70\,\mathrm{mm\,d^{-1}}$ for the urban area and $15\,\mathrm{mm\,d^{-1}}$ for the rural areas. Applying $70\,\mathrm{mm\,d^{-1}}$ of drainage capacity to the urbanized part of the study area (See Fig. 3) represents an average flow of $30.64\,\mathrm{m^3\,s^{-1}}$. This value seems coherent with the installed pumping capacity described above. Therefore, a drainage capacity map has been created using the values from Yu and T. J. Coulthard (2015) on the urban and non-urban areas defined by the GLC30 map (See Fig. 3). The artificial surfaces have been assigned a value of $2.917\,\mathrm{mm\,h^{-1}}$ and the remaining areas $0.625\,\mathrm{mm\,h^{-1}}$.

T. Coulthard and Frostick (2010) estimate that the soil was saturated due to the important rainfall prior to the studied event. Therefore, we examined two hypotheses. In the first one, we considered that the soil saturation prevents any infiltration, and the rate is $0\,\mathrm{mm\,h^{-1}}$. In the second hypothesis we took the infiltration rate to be constant in time and equal to the soil hydraulic conductivity, a view consistent with the Green–Ampt model. We estimated the conductivity with the help of the global soil database SoilGrids250m (Hengl et al., 2017). First, we calculated the average clay and sand values in the top 60 cm of soil and classified the soil according to textures definitions from the United States Department of Agriculture (USDA). Then we related the texture classes with typical values obtained from experiments

Preprints (www.preprints.org) | NOT PEER-REVIEWED | Posted: 29 August 2017 doi:10.20944/preprints201708.0101.v1

(Rawls et al., 1983). The resulting map has an average hydraulic conductivity of 3.57 mm h^{-1} on the study area.

For the Precipitation we compare two sources of information. The first one is the measurement from an uncalibrated rain gauge at the University of Hull (Yu and T. J. Coulthard, 2015). Its temporal resolution is of 1 h and it is considered uniform in space. The second one is a time-series of raster maps reconstructed using various rain gauges and a meteorological radar. Although radar rainfall provides spatial rainfall information, it fails to estimate the correct intensity, partly because it may be affected by different sources of errors. On the other hand, rain gauges can measure the point rainfall intensities more accurately, but are unable to provide information on the spatial rainfall distribution. Merging the two sources of rainfall data is recognised to improve the estimates (Goudenhoofdt and Delobbe, 2009; Haberlandt, 2007; Jewell and Gaussiat, 2015; Schuurmans et al., 2007; Wilson, 1970). The selected radar-gauge merging method is Kriging with External Drift (KED) (Chiles and Delfiner, 2012; Cressie, 2015). KED assumes the mean of the process (drift) as a linear function of external covariates. In this case, the only considered covariate is the radar rainfall.

For this event, we use the Weather radar rainfall composite product from the UK Met Office at 1 km and 5 min spatial and temporal resolutions (Harrison et al., 2009) and a series of rain gauges from the EA to create the raster time-series using KED. The radar rainfall product has been quality-controlled by the UK Met Office and it has been corrected for well-known sources of error in radar rainfall. Note that the urban area was mainly covered by the Hameldon Hill radar located more than 100km towards the West of the urban area. Figure 4 shows the map of accumulated precipitation together with the locations of the weather radar and rain gauges. Due to the distance of the radar from Hull, the actual radar rainfall spatial resolution above the study area is around 5 km. Furthermore, the radar rainfall had gaps in data during this event and therefore the missing time periods were interpolated using a nowcasting model (Liguori and M. A. Rico-Ramirez, 2014). Unfortunately some of the missing periods occurred during the time of heavy precipitation falling on the urban area. The spatial resolution of the resulting rainfall field is of 1 km. The radar rainfall scans were accumulated to produce a temporal resolution of 1 h. Figure 6 shows the evolution in time of the rainfall field generated by KED, while the mean hyetographs of each rainfall are compared in Fig. 5 (averaged over the urban area). Note that some time steps shown in Fig. 6 show a KED spatial rainfall resolution of 1 km due to the fact that the radar-gauge KED merging was performed at 1 km resolution and also because the nowcasting model to interpolate the missing time periods also runs at 1 km. The precipitated volumes during the event are 6.1 hm^3 and 5.9 hm^3 for the uniform rainfall and the KED rainfall, respectively.

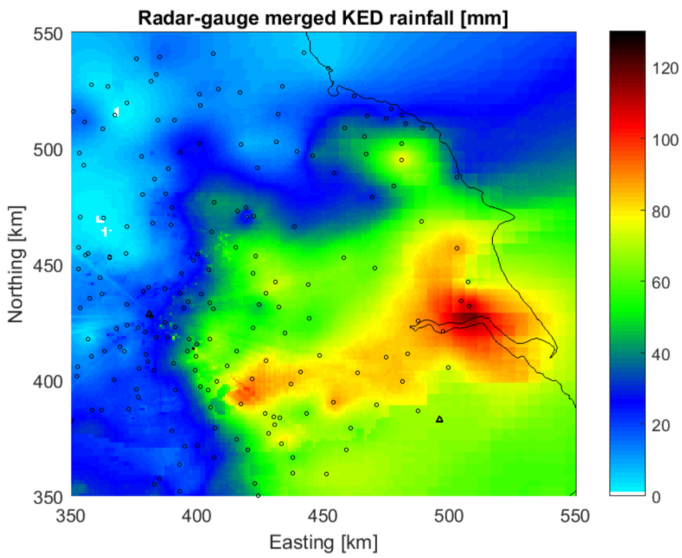

Figure 4: *Accumulated rainfall obtained from KED. Circles represent the rain gauges used. Triangles are the weather radars. Please note that during this event, only Hameldon Hill radar (located at the west of the region) was operating.*

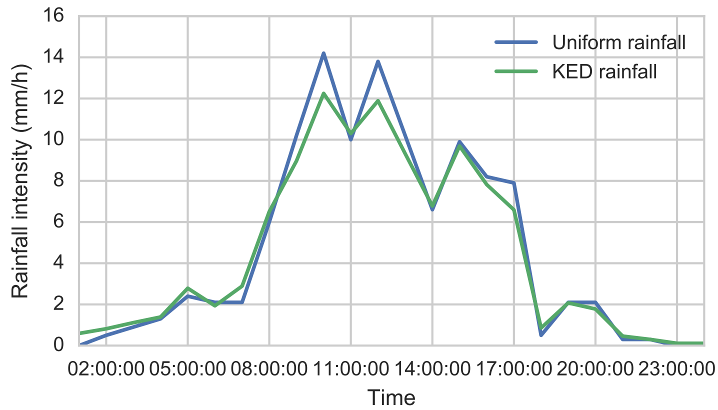

Figure 5: *Mean hyetographs above the study area.*

 doi:10.20944/preprints201708.0101.v1

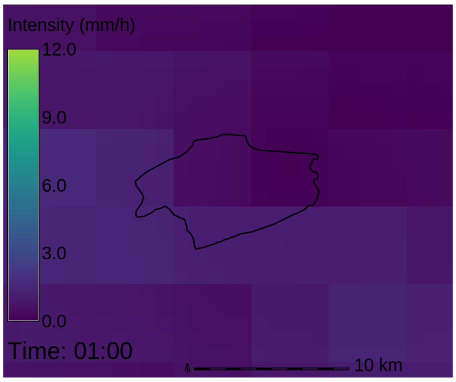

(a) *00:00–01:00*

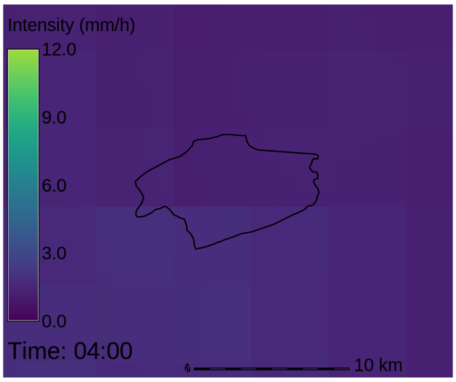

(b) *03:00–04:00*

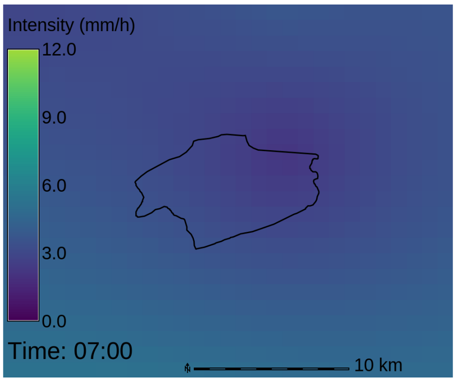

(c) *06:00–07:00*

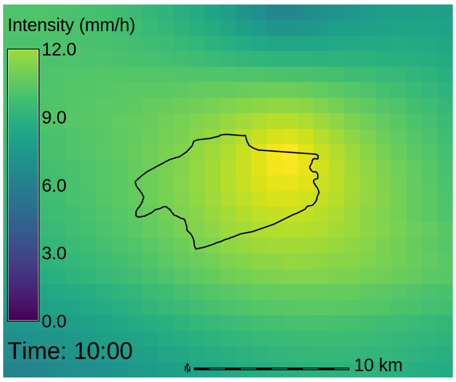

(d) *09:00–10:00*

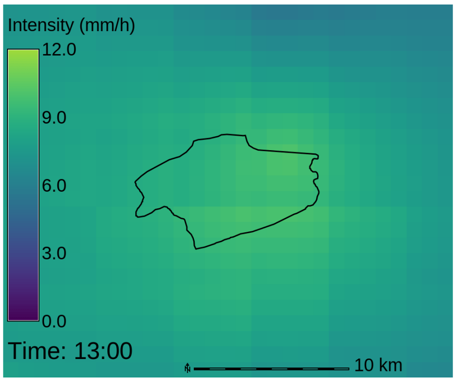

(e) *12:00–13:00*

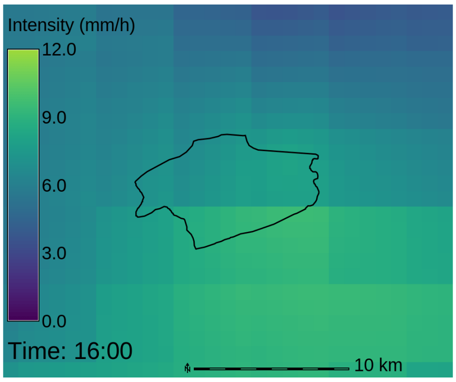

(f) *15:00–16:00*

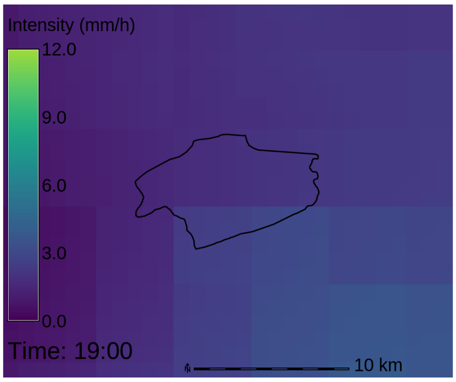

(g) *18:00–19:00*

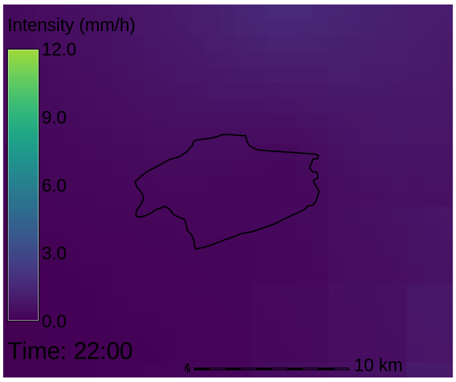

(h) *21:00–22:00*

Figure 6: *Evolution of rainfall intensity obtained with KED.*

 doi:10.20944/preprints201708.0101.v1

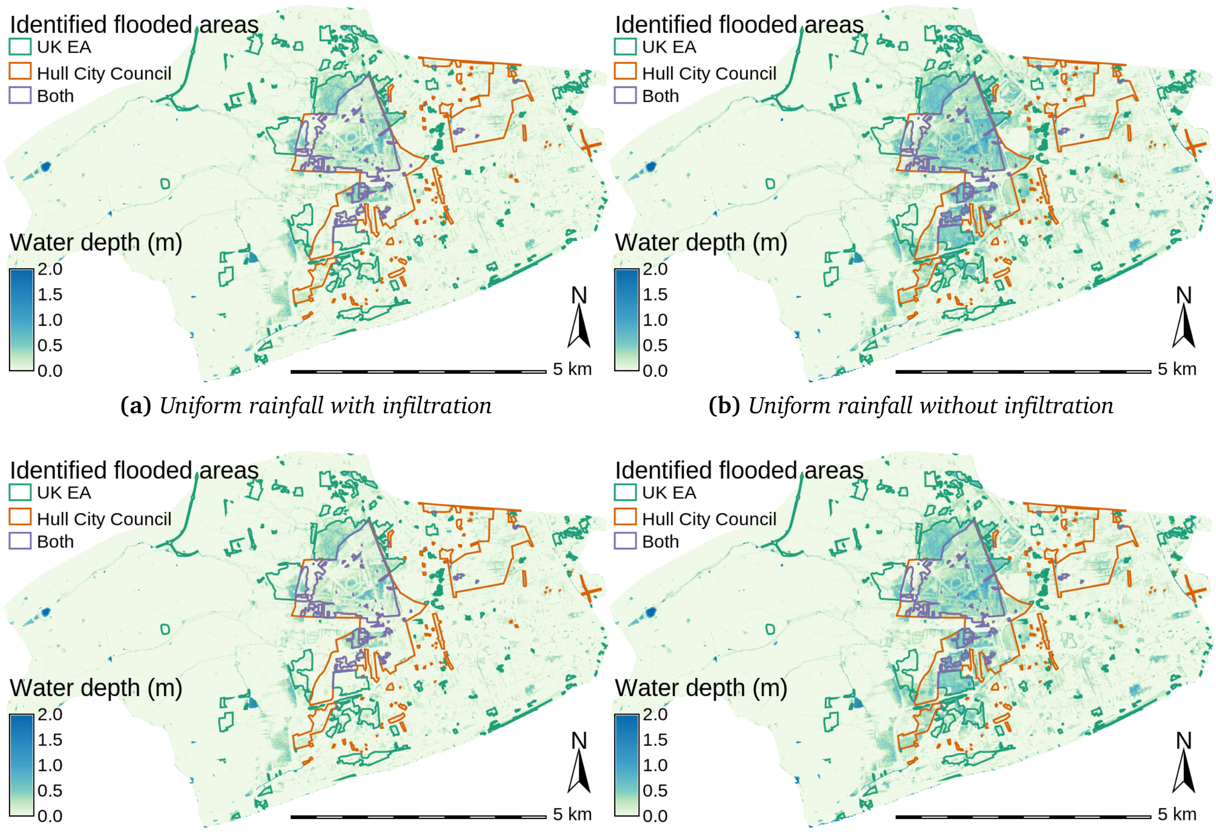

(a) *Uniform rainfall with infiltration*

(b) *Uniform rainfall without infiltration*

(c) *KED rainfall with infiltration*

(d) *KED rainfall without infiltration*

Figure 7: *Comparison between observed extents and maximum computed water depths.*

3 Results

We run a total of four simulations to assess all the combinations of parameters, which are KED and uniform precipitations and the consideration or not of the infiltration. We first examine the results from a qualitative point of view and then we subject them to a quantitative analysis.

3.1 Qualitative analysis

During the event, the water is accumulated in the lower part of the domain, which is the most urbanised. Figure 7 compares the computed maximum water levels with the observed extents. It shows that when infiltration is not considered, the model is able to identify the main flooded area observed by the two collecting entities, at the centre of the domain. For the other inundated parts, the comparison is more difficult because of the discrepancies between the observations of the EA and the HCC. On the other hand, it is clear that when considering the infiltration, the inundation volume is not sufficient to correctly represent most of the flooded areas.

Some differences in computed water level occurs between the simulation using the KED rainfall and the one using uniform rainfall. Figure 8 shows those differences in the case without infiltration. It could be noted that water levels obtained using KED are consistently lower than those using the uniform rainfall. The discrepancies are mostly between 5 cm to 10 cm, and is larger going eastward, with smaller areas where the differences reach 15 cm. This might be because this part of the inundation is mostly due to the overland flow coming from the upstream areas, and not from the local precipitation. The observed difference might therefore be due to the flood wave not reaching that far when the precipitated volume is lower.

Preprints (www.preprints.org) | NOT PEER-REVIEWED | Posted: 29 August 2017 doi:10.20944/preprints201708.0101.v1

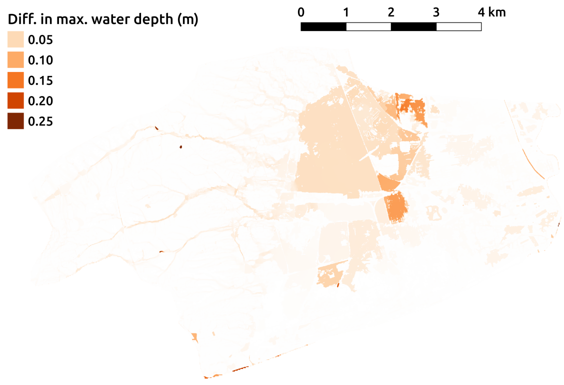

Figure 8: *Differences of maximum water depths between the results using uniform rainfall and those using Kriging with External Drift. Here is shown the case without infiltration.*

3.2 Quantitative analysis

We compare the resulting maps of maximum water levels with the identified flood extents. To do so, we classify each cell as flooded or dry using a threshold of computed water depth. There is no definite literature on the value of this threshold and it is mostly arbitrary (Wilks, 2011). Therefore, we use a series of values equally distributed from 0.6 cm to 30 cm. The generated binary maps shows a larger extent of inundation when the threshold is lower, and a smaller extent with a higher threshold. We then compare those generated maps to the observed extent maps using the Critical Success Index (CSI) as a skill evaluation score. Taking into account the differences between the two datasets of identified flooded areas (see Fig. 2), we decided to compare each computed extents to each individual observed extent and to a union of both observed extents. The results of this comparison are shown in Figure 9. Overall, the calculated CSI are quite weak, topping just above 35 % in the best case.

The CSI calculated against the union of extents are higher than when calculated with any of the two individual extents. This might give us an indication that the actual flooded area was larger than those identified by the EA or the HCC. Meanwhile, the CSI are higher without infiltration than when it is integrated. The differences in CSI between the KED and uniform rainfall are small when no infiltration at all is taken into account. However the use of uniform rainfall results in a higher higher peak CSI value. The differences between rainfall types are higher when the infiltration is considered. In that latter case, the uniform rainfall clearly represent better the actual event. On the other hand, the differences become minimal when infiltration is neglected.

4 Discussion and conclusions

First, we evaluate our results in light of those obtained by Yu and T. J. Coulthard (2015) that performed a sensitivity analysis and calibration of a similar model (FloodMap-HydroInundation2D, see Table 1) with the same event. They started by evaluating the sensitivity of the model to mesh resolution (10 and 20 m) and roughness (Manning's n equal to 0.01, 0.02, 0.03, 0.04 and 0.05 s m$^{-1/3}$). Subsequently, the authors performed a model calibration. They used a Manning's n of 0.03 s m$^{-1/3}$, chosen because it was within the range of theoretical values and a spatial resolution of 20 m to save on computation time. The authors used the hydraulic conductivity as a calibration parameter with tested values of 1, 2, 3, 4 and 5 mm h^{-1}. They rely on the "F statistic" and Root Mean Square Error (RMSE) to compare each results to a base simulation using a n of 0.01 s m$^{-1/3}$. The authors do not specify what they mean by "F statistic" nor indicates its formula. "F" is sometimes used in hydrology to designate the CSI (Stephens et al., 2014). In that case, Yu and T. J. Coulthard (2015) do not mention the threshold used to determine the wet/dry condition of each cell, which is necessary to employ a dichotomous score like the CSI. Yu and

Preprints (www.preprints.org) | NOT PEER-REVIEWED | Posted: 29 August 2017 doi:10.20944/preprints201708.0101.v1

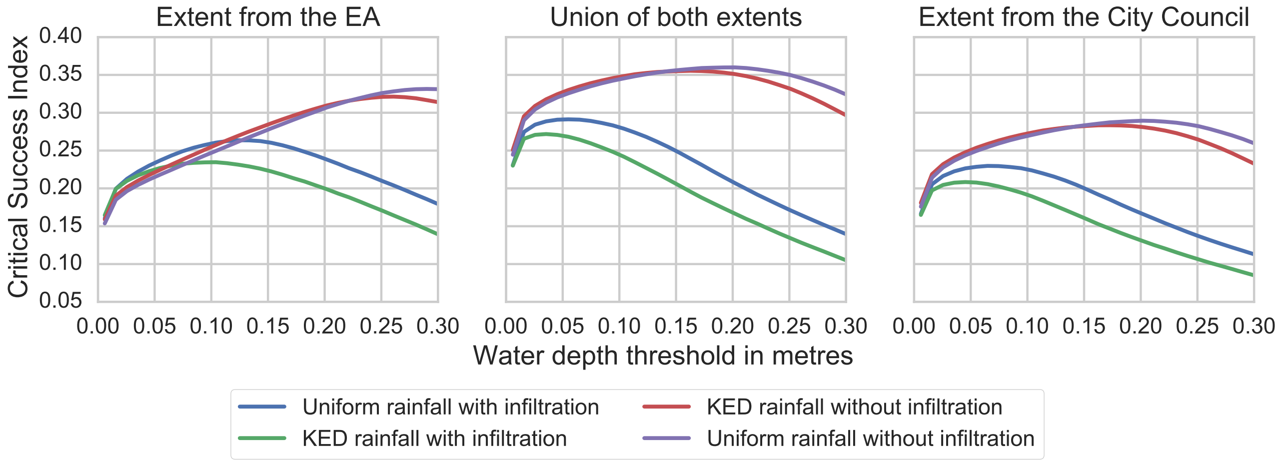

Figure 9: *Values of the Critical Success Index of each simulation results for a series of computed water depth thresholds.*

T. J. Coulthard (2015) found that the model was sensible to hydraulic conductivity and that a value of 3 mm h^{-1} was resulting in the highest "F" value, with 35 %.

The best value of CSI we find (See Fig.9) is indeed very similar to that "F" value, at slightly above 0.35. However, we achieved this CSI score by neglecting the infiltration, which contradicts the finding of Yu and T. J. Coulthard (2015). When we consider the infiltration, the CSI drops below 0.30. While the setting of the present study is very similar to the one of Yu and T. J. Coulthard (2015), some differences might explain those discrepancies in results.

First of all, we use here an infiltration rate that variate in space depending on the soil properties (see Section 2.2), whereas Yu and T. J. Coulthard (2015) use a uniform hydraulic In this study, we use a constant infiltration rate, which is consistent in a fully saturated soil with the Green–Ampt formula (4), as reported by Rawls et al. (1983). On the other hand, Yu and T. J. Coulthard (2015) use a variation of the Green–Ampt formula that neglects the state of saturation of the soil but takes into account the depth of pounding water overground. This results in a time-variating and non-uniform infiltration rate. Furthermore, when averaged across the whole area, the hydraulic conductivity used in this study is 3.57 mm h^{-1} when while the one selected by Yu and T. J. Coulthard (2015) is 3.0 mm h^{-1}.

Other factors could be taken into account. We do not consider the evapotranspiration, while Yu and T. J. Coulthard (2015) do. However, the amount involved (around 3 to 5 mm d^{-1}) are unlikely to create a big difference in an extreme event like the one studied here. Perhaps more importantly, the spatial resolution used for the calibration by Yu and T. J. Coulthard (2015) is 20 m, which might introduce more uncertainty than the 5 m resolution used in this paper.

Additionally, we obtain the highest values of CSI when comparing the computed extent with a union of both observations from the EA and HCC. This concurs with the assessment of T. Coulthard and Frostick (2010) that the actual flooded area might be more extended than reported by the public authorities.

Finally, while acknowledging the challenge of evaluating a computer model against such uncertain observations (see Section 2.2), Yu and T. J. Coulthard (2015) suggested that including the spatial variability of the rainfall might improve the capacity of the numerical model to reproduce the event. This assumption is in accordance with an abundant literature that indicates that spatial variability of rainfall is critical for urban flood modelling (Segond et al., 2007; Bruni et al., 2015; M. Rico-Ramirez et al., 2015; Cristiano et al., 2017).

In the present study however, we found that the inclusion of spatially-variable precipitation does not improve the capacity of the numerical model to reproduce the inundation event. This behaviour might be related to the flood volume necessary to reproduce the event. First, the precipitated volume of the KED rainfall is slightly lower than the one from the uniform rainfall (see Section 2.2). Second, the difference is accentuated when the infiltration process subtracts volume from the computational domain (see Fig. 9). This is an indication that the effective rainfall for this event might have been actually higher that the one modelled in this paper.

Additionally, the available radar data for this event comes from an equipment rather far from the study area. This results in an actual spatial resolution of 5 km and could induce bias in the rainfall measurement. Furthermore, there were missing time periods in the radar data that needed to be filled using nowcasting interpolation before preforming the KED radar-gauge merging. Finally, the rainfall event reproduced here is a large, slow-moving depression that affected a large part of the UK (T. Coulthard and Frostick, 2010). Due to the size of the study area, taking into account the spatial variability of the rainfall is likely to be more beneficial in case of convective events with more localised effects and when using sensors able to record those phenomenons with adequate accuracy.

This study shows that while many works has been published about the positive effects on urban flood modelling of integrating the spatial variability of rainfall, the benefits likely depend on the quality of the entry data, the type of the event and the size of the study area. Moreover, documentation of historical event is of critical importance to assess the capacity of a numerical model in a real world setting and uncertain data could jeopardise the model calibration process. More work is needed on the combination of better event data collection techniques and improved high-resolution precipitation data. Both could be achieved by the conjugation of traditional in-situ methods with remote-sensing.

Acknowledgements

The authors would like to thank the UK Met Office (radar rainfall requested at Met Office (2003).), and the Environment Agency (rain gauge data requested at http://environment-agency.gov.uk/) for providing some of the data sets used in this study. We thank Dr. Dapeng Yu from Loughborough University for kindly providing the DEM, the maps of observed flooded areas and the rain gauge records at the University of Hull. Laurent Courty extends his thanks the UNAM's Coordination of Postgraduate Studies for its support through a full doctoral scholarship.

Author Contributions

Adrián Pedrozo-Acuña and Laurent Courty designed the study. Laurent Courty performed the experiments and created most of the figures. Miguel Rico-Ramirez generated the KED rainfall field and Figure 4. All authors participated in the interpretation of the results and the redaction of the manuscript.

Conflicts of Interest

The authors declare no conflict of interest.

References

Almeida, Gustavo A. M. de and Paul David Bates (2013). "Applicability of the local inertial approximation of the shallow water equations to flood modeling". In: *Water Resources Research* 49.8, pp. 4833–4844. ISSN: 00431397. DOI: 10.1002/wrcr.20366.

Almeida, Gustavo A. M. de, Paul David Bates, et al. (2012). "Improving the stability of a simple formulation of the shallow water equations for 2-D flood modeling". In: *Water Resources Research* 48.5, pp. 1–14. ISSN: 00431397. DOI: 10.1029/2011WR011570.

Bates, Paul David, Matthew S. Horritt, and Timothy J. Fewtrell (2010). "A simple inertial formulation of the shallow water equations for efficient two-dimensional flood inundation modelling". In: *Journal of Hydrology* 387.1, pp. 33–45. ISSN: 00221694. DOI: 10.1016/j.jhydrol.2010.03.027. URL: http://dx.doi.org/10.1016/j.jhydrol.2010.03.027.

Bruni, G. et al. (2015). "On the sensitivity of urban hydrodynamic modelling to rainfall spatial and temporal resolution". In: *Hydrology and Earth System Sciences* 19.2. ISSN: 16077938. DOI: 10.5194/hess-19-691-2015.

Chen, Jun et al. (2014). "Global land cover mapping at 30m resolution: A POK-based operational approach". In: *ISPRS Journal of Photogrammetry and Remote Sensing* 103, pp. 7–27. ISSN: 09242716. DOI: 10.1016/j.isprsjprs.2014.09.002. URL: http://www.sciencedirect.com/science/article/pii/S0924271614002275.

Chiles, Jean-Paul and Pierre Delfiner (2012). *Geostatistics : modeling spatial uncertainty*. John Wiley & Sons, p. 726. ISBN: 9781118136171.

Chow, Ven Te (1959). *Open channel hydraulics*. McGraw-Hill Book Company, Inc; New York.

Coulthard, T.J. and L.E. Frostick (2010). "The Hull floods of 2007: implications for the governance and management of urban drainage systems". In: *Journal of Flood Risk Management* 3.3, pp. 223–231. ISSN: 1753318X. DOI: 10.1111/j.1753-318X.2010.01072.x. URL: http://doi.wiley.com/10.1111/j.1753-318X.2010.01072.x.

Courty, Laurent Guillaume, Adrián Pedrozo-Acuña, and Paul David Bates (2017). "Itzï (version 17.1): an open-source, distributed GIS model for dynamic flood simulation". In: *Geoscientific Model Development* 10.4, pp. 1835–1847. DOI: 10.5194/gmd-10-1835-2017. URL: http://www.geosci-model-dev.net/10/1835/2017/.

Cressie, Noel (2015). *Statistics for spatial data*. Revised Ed. John Wiley & Sons, p. 928. ISBN: 9781119115175.

Cristiano, Elena, Marie-claire ten Veldhuis, and Nick van de Giesen (2017). "Spatial and temporal variability of rainfall and their effects on hydrological response in urban areas – a review". In: *Hydrology and Earth System Sciences* 21.7, pp. 3859–3878. ISSN: 1607-7938. DOI: 10.5194/hess-21-3859-2017. URL: https://www.hydrol-earth-syst-sci.net/21/3859/2017/.

Ercan, Mehmet B. and Jonathan L. Goodall (2013). "Estimating Watershed-Scale Precipitation by Combining Gauge- and Radar-Derived Observations". In: *Journal of Hydrologic Engineering* 18.8, pp. 983–994. ISSN: 1084-0699. DOI: 10.1061/(ASCE)HE.1943-5584.0000687. URL: http://ascelibrary.org/doi/10.1061/%28ASCE%29HE.1943-5584.0000687.

Goudenhoofdt, E. and L. Delobbe (2009). "Evaluation of radar-gauge merging methods for quantitative precipitation estimates". In: *Hydrology and Earth System Sciences* 13.2, pp. 195–203. ISSN: 1607-7938. DOI: 10.5194/hess-13-195-2009. URL: http://www.hydrol-earth-syst-sci.net/13/195/2009/.

Haberlandt, Uwe (2007). "Geostatistical interpolation of hourly precipitation from rain gauges and radar for a large-scale extreme rainfall event". In: *Journal of Hydrology* 332.1-2, pp. 144–157. ISSN: 00221694. DOI: 10.1016/j.jhydrol.2006.06.028. URL: http://www.sciencedirect.com/science/article/pii/S0022169406003416.

Harrison, D. L., R. W. Scovell, and M. Kitchen (2009). "High-resolution precipitation estimates for hydrological uses". In: *Proceedings of the Institution of Civil Engineers - Water Management* 162.2, pp. 125–135. ISSN: 1741-7589. DOI: 10.1680/wama.2009.162.2.125. URL: http://www.icevirtuallibrary.com/doi/10.1680/wama.2009.162.2.125.

Hengl, Tomislav et al. (2017). "SoilGrids250m: Global Gridded Soil Information Based on Machine Learning". In: *PLOS One* 12, pp. 1–40. DOI: 10.1371/journal.pone.0169748.

Hill, David et al. (2014). "Sensing and Cyberinfrastructure for Smarter Water Management: The Promise and Challenge of Ubiquity". In: *Journal of Water Resources Planning and Management* 140.7, p. 01814002. ISSN: 0733-9496. DOI: 10.1061/(ASCE)WR.1943-5452.0000449. URL: http://ascelibrary.org/doi/10.1061/%28ASCE%29WR.1943-5452.0000449.

Hirabayashi, Yukiko et al. (2013). "Global flood risk under climate change". In: *Nature Climate Change* 3.9, pp. 816–821. ISSN: 1758-678X. DOI: 10.1038/nclimate1911. URL: http://www.nature.com/doifinder/10.1038/nclimate1911.

Hunter, N. M. et al. (2008). "Benchmarking 2D hydraulic models for urban flooding". In: *Proceedings of the ICE - Water Management* 161.1, pp. 13–30. ISSN: 1741-7589. DOI: 10.1680/wama.2008.161.1.13. URL: http://eprints.whiterose.ac.uk/77249/.

Jewell, Sharon A. and Nicolas Gaussiat (2015). "An assessment of kriging-based rain-gauge-radar merging techniques". In: *Quarterly Journal of the Royal Meteorological Society* 141.691, pp. 2300–2313. ISSN: 00359009. DOI: 10.1002/qj.2522. URL: http://doi.wiley.com/10.1002/qj.2522.

Leandro, J., A. Schumann, and A. Pfister (2016). "A step towards considering the spatial heterogeneity of urban key features in urban hydrology flood modelling". In: *Journal of Hydrology* 535. ISSN: 00221694. DOI: 10.1016/j.jhydrol.2016.01.060.

Liguori, Sara and Miguel Angel Rico-Ramirez (2014). "A review of current approaches to radar-based quantitative precipitation forecasts". In: *International Journal of River Basin Management* 12.4, pp. 391–402. ISSN: 1571-5124. DOI: 10.1080/15715124.2013.848872. URL: http://www.tandfonline.com/doi/abs/10.1080/15715124.2013.848872.

Met Office (2003). *1 km Resolution UK Composite Rainfall Data from the Met Office Nimrod System*. URL: http://catalogue.ceda.ac.uk/uuid/27dd6ffba67f667a18c62de5c3456350.

Nesbitt, Stephen W. and Alison M. Anders (2009). "Very high resolution precipitation climatologies from the Tropical Rainfall Measuring Mission precipitation radar". In: *Geophysical Research Letters* 36.15, n/a–n/a. ISSN: 00948276. DOI: 10.1029/2009GL038026. URL: http://doi.wiley.com/10.1029/2009GL038026.

Neteler, Markus et al. (2012). "GRASS GIS: A multi-purpose open source GIS". In: *Environmental Modelling & Software* 31, pp. 124–130.

Rawls, Walter J., Donald L. Brakensiek, and Norman Miller (1983). "Green-Ampt infiltration parameters from soils data". en. In: *Journal of Hydraulic Engineering* 109.1, pp. 62–70. ISSN: 0733-9429. DOI: 10.1061/(ASCE)0733-9429(1983)109:1(62).

Rico-Ramirez, M.A., S. Liguori, and A.N.A. Schellart (2015). "Quantifying radar-rainfall uncertainties in urban drainage flow modelling". In: *Journal of Hydrology* 528, pp. 17–28. ISSN: 00221694. DOI: 10.1016/j.jhydrol.2015.05.057.

Schuurmans, J. M. et al. (2007). "Automatic Prediction of High-Resolution Daily Rainfall Fields for Multiple Extents: The Potential of Operational Radar". In: *Journal of Hydrometeorology* 8.6, pp. 1204–1224. ISSN: 1525-755X. DOI: 10.1175/2007JHM792.1. URL: http://journals.ametsoc.org/doi/abs/10.1175/2007JHM792.1.

Segond, Marie-Laure, Howard S. Wheater, and Christian Onof (2007). "The significance of spatial rainfall representation for flood runoff estimation: A numerical evaluation based on the Lee catchment, UK". In: *Journal of Hydrology* 347.1, pp. 116–131. ISSN: 00221694. DOI: 10.1016/j.jhydrol.2007.09.040.

Seo, D.-J. (1998). "Real-time estimation of rainfall fields using radar rainfall and rain gage data". In: *Journal of Hydrology* 208.1-2, pp. 37–52. ISSN: 00221694. DOI: 10.1016/S0022-1694(98)00141-3. URL: http://linkinghub.elsevier.com/retrieve/pii/S0022169498001413.

Smith, James A., Mary Lynn Baeck, et al. (2007). "Radar rainfall estimation for flash flood forecasting in small urban watersheds". In: *Advances in Water Resources* 30.10, pp. 2087–2097. ISSN: 03091708. DOI: 10.1016/j.advwatres.2006.09.007. URL: http://linkinghub.elsevier.com/retrieve/pii/S0309170807000553.

Smith, James A. and Witold F. Krajewski (1993). "A modeling study of rainfall rate-reflectivity relationships". In: *Water Resources Research* 29.8, pp. 2505–2514. ISSN: 00431397. DOI: 10.1029/93WR00962. URL: http://doi.wiley.com/10.1029/93WR00962.

Stephens, Elisabeth, Guy Jean-Pierre Schumann, and Paul David Bates (2014). "Problems with binary pattern measures for flood model evaluation". In: *Hydrological Processes* 28.18, pp. 4928–4937. ISSN: 08856087. DOI: 10.1002/hyp.9979. URL: http://doi.wiley.com/10.1002/hyp.9979.

Velasco-Forero, Carlos A. et al. (2009). "A non-parametric automatic blending methodology to estimate rainfall fields from rain gauge and radar data". In: *Advances in Water Resources* 32.7, pp. 986–1002. ISSN: 03091708. DOI: 10.1016/j.advwatres.2008.10.004. URL: http://linkinghub.elsevier.com/retrieve/pii/S0309170808001760.

Vojinović, Zoran and Michael B. Abbott (2012). *Flood risk and social justice : from quantitative to qualitative flood risk assessment and mitigation*. IWA Publishing, p. 563. ISBN: 1843393875.

 doi:10.20944/preprints201708.0101.v1

Wilks, D.S. (2011). "Forecast Verification". In: *Statistical Methods in the Atmospheric Sciences*. Elsevier, pp. 301–394. ISBN: 978-0-12-385022-5. DOI: 10.1016/B978-0-12-385022-5.00008-7. URL: http://linkinghub.elsevier.com/retrieve/pii/B9780123850225000087.

Wilson, James W. (1970). "Integration of Radar and Raingage Data for Improved Rainfall Measurement". In: *Journal of Applied Meteorology* 9.3, pp. 489–497. ISSN: 0021-8952. DOI: 10.1175/1520-0450(1970)009<0489:IORARD>2.0.CO;2. URL: http://journals.ametsoc.org/doi/abs/10.1175/1520-0450%281970%29009%3C0489%3AIORARD%3E2.0.CO%3B2.

Yu, Dapeng and Tom J. Coulthard (2015). "Evaluating the importance of catchment hydrological parameters for urban surface water flood modelling using a simple hydro-inundation model". In: *Journal of Hydrology* 524, pp. 385–400. ISSN: 00221694. DOI: 10.1016/j.jhydrol.2015.02.040.